JCTC Journal of Chemical Theory and Computation

Article

pubs.acs.org/JCTC

Elucidating the Molecular Origin of Hydrolysis Energy of Pyrophosphate in Water

Jooyeon Hong,[†] Norio Yoshida,[‡] Song-Ho Chong,[†] Chewook Lee,[†] Sihyun Ham,*[,†] and Fumio Hirata*[,§]

[†]Department of Chemistry, Sookmyung Women's University, Cheongpa-ro 47-gil 100, Yongsan-Ku, Seoul 140-742, Korea

[‡]Department of Chemistry, Faculty of Sciences, Kyusyu University, Fukuoka 812-8581, Japan

[§]Department of Theoretical Molecular Science, Institute for Molecular Science, Okazaki 444-8585, Japan

Supporting Information

ABSTRACT: The molecular origin of the energy produced by the ATP hydrolysis has been one of the long-standing fundamental issues. A classical view is that the negative hydrolysis free energy of ATP originates from intramolecular effects connected with the backbone P−O bond, so called "high-energy bond". On the other hand, it has also been recognized that solvation effects are essential in determining the hydrolysis free energy. Here, using the 3D-RISM-SCF (three-dimensional reference interaction site model self-consistent field) theory that integrates the *ab initio* quantum chemistry method and the statistical mechanical theory of liquids, we investigate the molecular origin of hydrolysis free energy of pyrophosphate, an ATP analogue, in water. We demonstrate that our theory quantitatively reproduces the experimental results without the use of empirical parameters. We clarify the crucial role of water in converting the hydrolysis free energy in the gas phase determined solely by intramolecular effects, which ranges from endothermic, thermoneutral, to highly exothermic depending on the charged state of pyrophosphate, into moderately exothermic in the aqueous phase irrespective of the charged state as observed in experimental data. We elucidate that this is brought about by different natures of solute−water interactions depending on the charged state of solute species: the hydration free energy of low-charged state is mainly subjected to short-range hydrogen-bonds, while that of high-charged state is dominated by long-range electrostatic interactions. We thus provide unambiguous evidence on the critical role of water in determining the ATP hydrolysis free energy.

INTRODUCTION

ATP conversion into ADP, called ATP hydrolysis, is the source of energy in all biological functions.[1] It has originally been proposed and is still conceived widely that the negative hydrolysis free energy is associated with the backbone P−O bond in ATP, so-called "high-energy" P−O bond.[2−13] On the other hand, the critical importance of solvation effects has also been recognized in determining the hydrolysis free energy.[14−20] George and co-workers proposed that the hydrolysis free energies of phosphate compounds are determined mainly by the differences in solvation free energies of reactants and products, and not by intramolecular effects.[14] Subsequent experimental investigation in aqueous media containing different concentrations of organic solvents has shown that the hydrolysis free energy depends strongly on the water activity.[16] However, the joint role of special intramolecular properties connected with the P−O bond and hydration effects that vary significantly with the solute charged state remains to be revealed. For example, the hydrolysis free energies of various kinds of phosphate compounds in aqueous phase are experimentally found to be comparable,[14] despite the large difference in sign and magnitude for the gas-phase values.[7] Thus, the role of water, though its significance is recognized, should largely vary for different solute species, but such an effect has yet been comprehensively understood at the molecular level.

Most of the previous theoretical studies employed an implicit solvation model such as the polarizable continuum model to understand the role of water and solvation free energy of phosphate compounds. Reliable calculations of solutes in solution must however take into account not only bulk electrostatics (i.e., long-range electrostatic polarization effects) but also shorter-range effects such as the free energy of cavity formation, dispersion, and solvent structural effects, the latter including both hydrogen bonding and exchange repulsion effects.[21] Recently, a microsolvation-continuum approach was applied to compute solvation free energies of phosphate compounds since the simple polarizable continuum model was found to be unable to yield accurate solvation free energies.[22] However, the treatment requires an empirical determination of the optimal number of water molecules to be explicitly handled in order to reproduce experimental values of the hydration free energies. Nevertheless, this work pointed out a necessity of molecular treatment of solvation effects in handling the phosphate compounds.

Here we investigate the molecular origin of hydrolysis free energy of a model compound of ATP, pyrophosphate, in water using the 3D-RISM-SCF (three-dimensional reference interaction site model self-consistent field) theory that integrates the *ab initio* quantum chemistry method and the statistical mechanical theory of liquids.[23−25] The theory treats the electronic structure of solute and the statistical solvent distribution around it in a self-consistent manner, and properly accounts for chemical specificities of solute−water interactions such as hydrogen bonding similarly to molecular simulations

Received: February 4, 2012
Published: June 3, 2012

   dx.doi.org/10.1021/ct300099e | *J. Chem. Theory Comput.* 2012, 8, 2239−2246

with explicit solvent. We apply this method to four different charged states of pyrophosphate for which experimental data for hydrolysis free energies are available. By performing the calculations for the reaction free energies both in the gas phase and in the aqueous phase without the use of any empirical parameters, we quantitatively and unambiguously demonstrate the role of water in the hydrolysis of pyrophosphate. In particular, we clarify different natures of solute−water interactions depending on the charged state of pyrophosphate. We argue that such differences explain why the experimental results for the aqueous-phase hydrolysis free energies are moderately exothermic irrespective of the charged state of pyrophosphate.

RESULTS AND DISCUSSION

Hydrolysis Free Energies. For the four possible charged states of pyrophosphates (see Scheme 1), the computed

Scheme 1. Schematic Description of the Hydrolysis Reaction of Pyrophosphate for the Four Possible Charged States

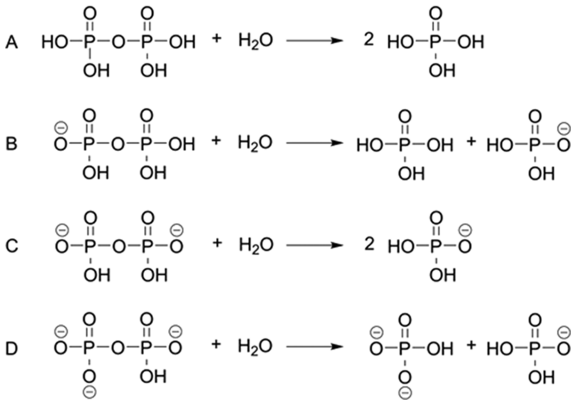

reaction free energies of the hydrolysis reactions are summarized and compared with experimental data in Table 1.

Table 1. Reaction Free Energies in the Gas Phase and in the Aqueous Phase at 298.15 K and 1.0 atm Computed by DFT at the B3LYP/6-31+(d) Level and the 3D-RISM-SCF Theory with Units in kcal/mol

reaction	gas phase (DFT)	aqueous phase (3D-RISM-SCF)	exptl[a]
A	−1.7	−8.9	−9.5
B	21.3	−6.2	−7.5
C	−56.6	−8.1	−7.7
D	−119.5	−7.7	−7.1

[a]Experimental values from ref 14.

Components of the gas-phase reaction free energies, i.e., reaction enthalpies and entropies, are listed in Table 2. The gas-phase geometries computed at the B3LYP/6-31+G(d) level are shown in Figure 1. As shown in Figure 1, the pyrophosphate molecules display maximized hydrogen bondings in a gas phase, and the average hydrogen bond distance is computed to be decreased as the total charge of pyrophosphate becomes more negative. In the gas phase, the hydrolysis reaction is close to thermoneutral for $H_4P_2O_7$ (A), endothermic for the mono-anionic $H_3P_2O_7^-$ (B), and exothermic for the dianionic $H_2P_2O_7^{2-}$ (C) and the trianionic $HP_2O_7^{3-}$ (D). The results in the gas phase can be explained in terms of the localization of

Table 2. Gas-Phase Reaction Free Energies (in kcal/mol), Enthalpies (in kcal/mol), and Entropies (Multiplied by the Temperature, in kcal/mol) at 298.15 K and 1.0 atm Computed by DFT at the B3LYP/6-31+G(d) Level

reaction	ΔG_{gas}	ΔH_{gas}	$T\Delta S_{gas}$
A	−1.7	1.4	3.1
B	21.3	24.6	3.3
C	−56.6	−53.1	3.5
D	−119.5	−117.8	1.7

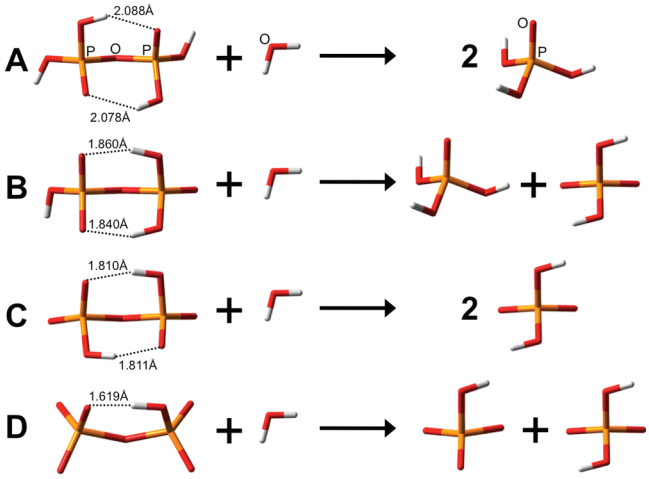

Figure 1. Optimized geometries in the gas phase of the reactants and products of the reactions A−D computed by DFT at the B3LYP/6-31+G(d) level. The dotted line and the number (in Å) denote hydrogen bonding and its distance, respectively.

excess electrons in a molecule and of the Coulomb repulsions among those electrons. In case A, the reaction free energy is vanishingly small because there is no excess electron either in the reactant or product states. In case B, the reaction becomes endothermic because an excess electron is localized in a phosphate molecule in the product. In cases C and D, the reaction becomes exothermic because excess electrons are localized more in the reactants causing electrostatic repulsion between negatively charged sites of pyrophosphates than in the products. Overall, the gas-phase hydrolysis free energies are significantly dependent on the reactant charged states. It is noted that the gas-phase reaction free energies (ΔG_{gas}) are mainly determined by the enthalpy term (ΔH_{gas}), and the relative contribution of the entropy term ($T\Delta S_{gas}$) is rather small at 298.15 K and 1.0 atm except for reaction A (Table 2). Nevertheless, the gas-phase hydrolysis free energy results are greatly deviated from the experimental data in which the hydrolysis reaction is moderately exothermic regardless of the reactant charged states.[14]

To obtain the hydrolysis free energy of pyrophosphates in the aqueous phase, we performed the 3D-RISM-SCF calculations[23−25] for all molecular species in Scheme 1. The optimized geometries computed by the 3D-RISM-SCF theory are displayed in Figure 2. Compared to the gas-phase geometries, the computed structure for the neutral species of $H_4P_2O_7$ (A) in the aqueous phase shows the most distinctive difference among pyrophosphates by having no intramolecular hydrogen bonding. Since the hydrogen atoms in $H_4P_2O_7$ (A) are free from forming H-bonding with phosphate oxygens, they are available to make H-bonding to solvent water in the

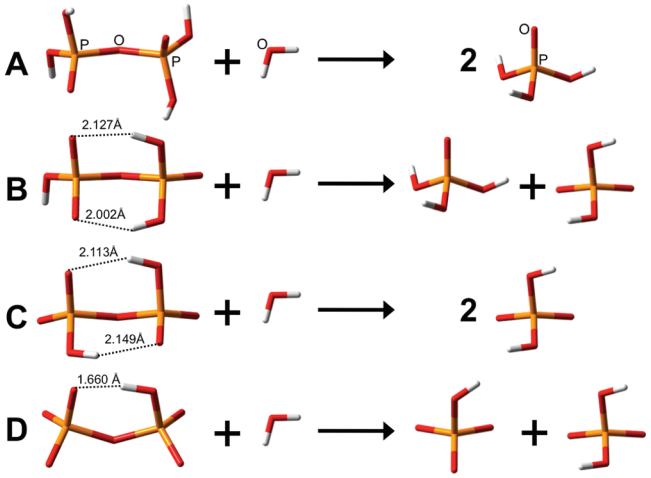

Figure 2. Optimized geometries in the aqueous phase of the reactants and products of the reactions A–D computed by the 3D-RISM-SCF theory. The dotted line and the number (in Å) denote hydrogen bonding and its distance, respectively.

aqueous phase. Negatively charged pyrophosphates display intramolecular hydrogen bonding whose distances are slightly more elongated than the corresponding ones in the gas phase geometries.

As shown in Table 1, the aqueous phase hydrolysis free energies for the reactions A–D show excellent agreement with those from the experiments. The agreement is attributed to the proper account of solvent effect based on the 3D-RISM-SCF theory. Comparing the 3D-RISM-SCF theory results with the gas phase results, some interesting aspects of the solvent effect are revealed. In particular, the solvent effect makes the hydrolysis reaction to be moderately exothermic in the aqueous phase, around 8 kcal/mol, for all the charged states of the pyrophosphates. This indicates that the role of water significantly varies with different charged state of phosphate compounds.

There are two sources in the free energy changes of the solute molecules due to hydration. The first of those is so-called "electronic reorganization energy" (δE) which originates from a distortion of the electronic structure due to the electrostatic field produced by the solvent. The other source is the excess chemical potential or so-called "solvation free energy" ($\delta\mu$) which originates from the solute–solvent interaction and the structural reorganization of the solvent. Summarized in Table 3 are the two contributions to the free energy change due to the solvent effect in the reactant and product states. It is found that the solvation free energy dominates over the electronic reorganization energy in all the dissociated states of the phosphates. In the case of lower charged states (reactions A and B), the products are more stabilized than the reactants. This converts the reaction from "thermoneutral" or "endothermic" in the gas phase to "exothermic" in water. On the other hand, in the case of higher charged states (reactions C and D) of the pyrophosphates, the reactants are stabilized by the solvent more dramatically than the products, making the reaction which is "highly exothermic" in the gas phase to be "moderately exothermic" in the aqueous phase.

Table 3. Solvation Contributions (Electronic Reorganization Energy δE and Solvation Free Energy $\delta\mu$) to the Reaction Free Energy Computed by the 3D-RISM-SCF Theory with Units in kcal/mol

	reactants		products	
reaction	δE	$\delta\mu$	δE	$\delta\mu$
A	8.2	−27.0	8.2	−32.6
B	6.7	−74.4	13.9	−113.7
C	5.8	−224.1	19.6	−194.8
D	9.7	−478.3	21.8	−385.2

Table 4 lists the components of the aqueous-phase free energy (G_{aq}) for each solute species. It is distinct that the solvation free energies ($\delta\mu$) for the higher charged states have much bigger negative values than those for the lower charged states. The excess electrons in more highly negative charged pyrophosphates, characterized by the higher gas-phase energy (E_{gas}), are much more stabilized by the hydration ($\delta\mu$), and taking properly into account such a degree of stabilization by hydration leads to quantitative agreement with the experimental data as shown in Table 1.

Table 4. Aqueous-Phase Free Energy G_{aq}, Solvation Free Energy $\delta\mu$, Electronic Reorganization Energy δE, Gas-Phase Energy E_{gas}, and Kinetic Energy G_{kin} of Reactant and Product Species Computed by the 3D-RISM-SCF Theory with Units in kcal/mol

	G_{aq}	$\delta\mu$	δE	E_{gas}	G_{kin}
H_3PO_4	−404 071.5	−16.3	4.1	−404 093.3	34.0
$H_2PO_4^-$	−403 824.8	−97.4	9.8	−403 763.7	26.5
HPO_4^{2-}	−403 563.8	−287.8	12.0	−403 306.6	18.6
$H_4P_2O_7$	−760 211.3	−19.5	6.0	−760 250.8	53.0
$H_3P_2O_7^-$	−75 967.2	−66.9	4.5	−759 950.4	45.6
$H_2P_2O_7^{2-}$	−759 718.6	−216.6	3.6	−759 543.7	38.1
$HP_2O_7^{3-}$	−759 458.1	−470.8	7.5	−759 024.4	29.6
H_2O	−47 922.9	−7.5	2.2	−47 932.6	15.0

Molecular Origin of the Reaction Free Energy. Depicted in Figure 3 are the three-dimensional distributions of water oxygen (O) and hydrogen (H) around all the solute species concerned with the reactions, which are in the different charged states. We also show in Figure 4 the radial distribution functions of O and H of solvent water around the phosphate species: the corresponding figures for the pyrophosphate species are presented in Figures S1–S4 of the Supporting Information. These figures exhibit quite characteristic hydration patterns depending on the charged states of the phosphates.

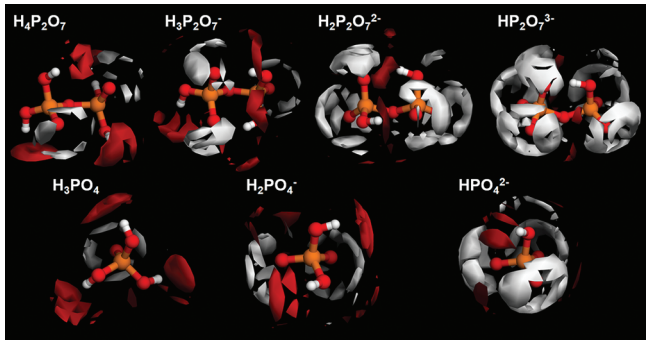

Figure 3. Spatial distribution functions of solvent water around the reactants and products. Distributions of oxygen and hydrogen of solvent water are red and gray, respectively.

dx.doi.org/10.1021/ct300099e | J. Chem. Theory Comput. 2012, 8, 2239–2246

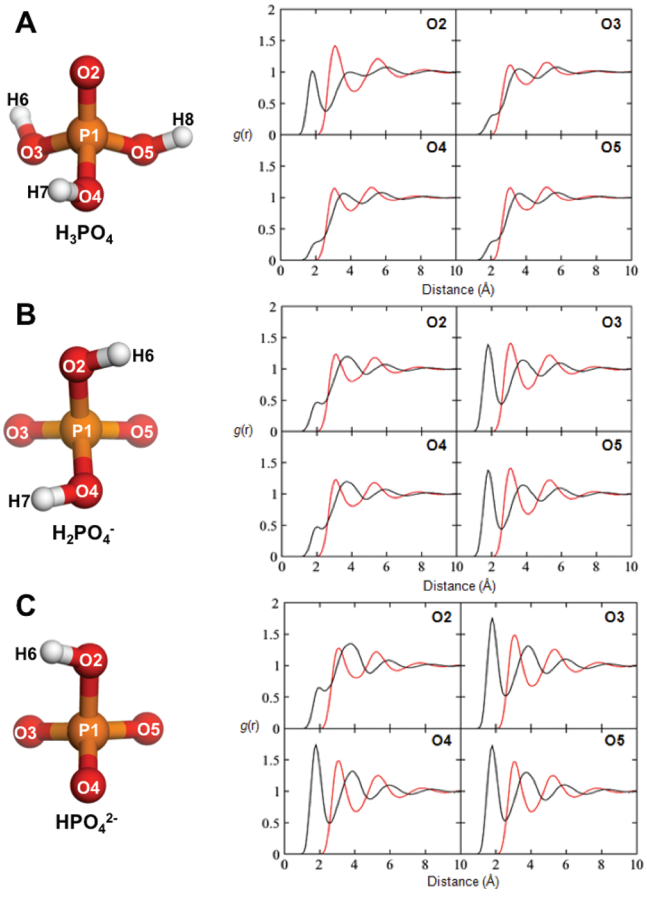

Figure 4. Radial distribution functions for (A) H_3PO_4, (B) $H_2PO_4^-$, and (C) HPO_4^{2-}. Radial distribution functions are evaluated by orientational averaging of the spatial distribution functions shown in Figure 3. The center of orientational averaging is indicated in each panel. Red and black curves denote the distribution functions of oxygen and hydrogen of solvent water, respectively. In the molecular model, oxygen, hydrogen, and phosphorus are red, white, and orange, respectively.

When a phosphate is not dissociated or does not have a net charge as in H_3PO_4 and $H_4P_2O_7$, the phosphate is primarily hydrated by water-oxygen through hydrogen-bonds. Although there is some distribution attributed to water-hydrogen around the oxygen atoms in phosphates, it is minor. Since reaction A is almost thermoneutral in the gas phase, the reaction free energy of −8.9 kcal/mol in the aqueous phase mainly comes from the difference in the short-range solute−solvent interactions between the reactants and products, including the energy of cavity formation, hydrogen-bond strength, and steric effect. When the phosphates have one negative charge as in $H_2PO_4^-$ and $H_3P_2O_7^-$, the hydration patterns are observed to be different, especially for $H_2PO_4^-$ where the distributions of water-hydrogen appear around negatively charged oxygen atoms in $H_2PO_4^-$ (Figures 3 and 4B). While the first peak height is somewhat underestimated, the features of the radial distribution functions for $H_2PO_4^-$ displayed in Figure 4B, such as a peak in the region of 1.5−2.0 Å and a minimum at 2.3−2.5 Å indicative of the hydrogen bonding, are in good agreement with the ones from the previous molecular dynamics simulations.[26] This hydration difference between the reactants and products due to the short-range interactions in reaction B converts the reaction from endothermic in the gas phase to be exothermic in the aqueous phase.

When the phosphates have multiple negative charges as in HPO_4^{2-}, $H_2P_2O_7^{2-}$, and $HP_2O_7^{3-}$, the hydration patterns are dramatically changed as conspicuous distributions of water-hydrogen appear around solute oxygen atoms (Figure 3). The increasing peak height of the radial distribution functions on going from $H_2PO_4^-$ to HPO_4^{2-} (Figure 4B,C) is also in agreement with the previous molecular dynamics simulation results.[26] When these phosphates have multiple negative charges, the long-range electrostatic interactions become critical in determining their hydration free energies. To quantify such an effect, we consider the electrostatic contribution to the hydration free energy $\delta\mu_q$, defined as the difference between the hydration free energy of the original solute molecule ($\delta\mu$) and the one ($\delta\mu_0$) in which the solute−solvent electrostatic interaction is turned off, $\delta\mu_q = \delta\mu - \delta\mu_0$. Its magnitude is

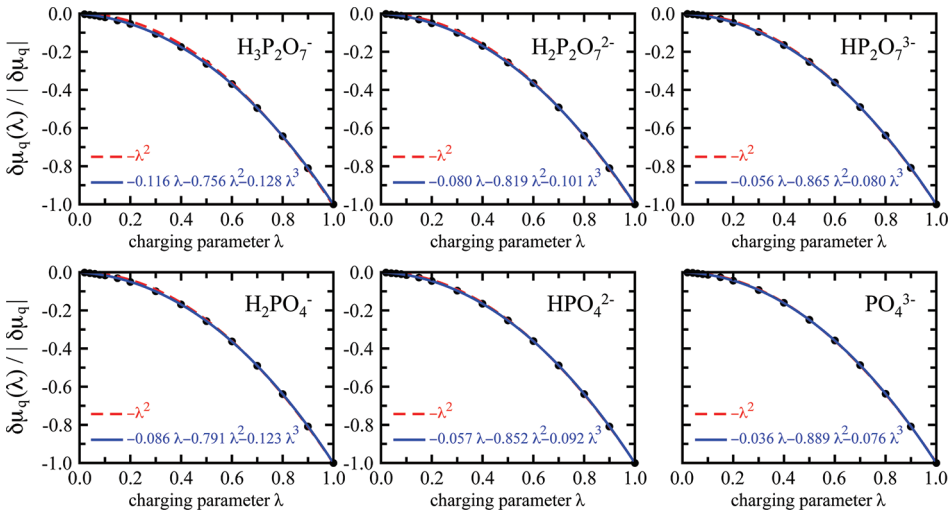

Figure 5. Normalized electrostatic contribution to the hydration free energy $\delta\mu_q(\lambda)/|\delta\mu_q|$ as a function of the charging parameter λ (●, calculated for λ = 0.02, 0.04, 0.06, 0.08, 0.10, 0.15, 0.20, 0.30, 0.40, 0.50, 0.60, 0.70, 0.80, 0.90, and 1.00). Deviation from the quadratic dependence, $-\lambda^2$ (red ---), appears for these systems, which however becomes smaller for higher charged species. Blue solid curve denotes the fit by $\xi_1\lambda - \xi_2\lambda^2 + \xi_3\lambda^3$ with the coefficients ξ_1, ξ_2, and ξ_3 specified in each panel.

determined by the fluctuation of the solute−solvent electrostatic interaction V_{elec}.[27,28] In fact, when the solute−solvent electrostatic interaction is scaled by a parameter λ, the resulting electrostatic contribution to the hydration free energy $\delta\mu_q(\lambda)$ is given by $\delta\mu_q(\lambda)/|\delta\mu_q| = \xi_1\lambda - \xi_2\lambda^2 + \xi_3\lambda^3 + \ldots$ (see Methods section). Here, $\xi_1 = \langle V_{elec}\rangle_0/|\delta\mu_q|$, $\xi_2 = \beta\langle\delta V_{elec}^2\rangle_0/(2|\delta\mu_q|)$, $\xi_3 = \beta^2\langle\delta V_{elec}^3\rangle_0/(6|\delta\mu_q|)$ with $\delta V_{elec} = V_{elec} - \langle V_{elec}\rangle_0$ and $\beta^{-1} = k_BT$. $\langle\cdots\rangle_0$ denotes the ensemble average over the states in which V_{elec} is turned off. Since V_{elec} is long-ranged, and hence, is a sum of many contributions, its distribution function is expected to be well approximated by Gaussian. When the distribution function of V_{elec} is Gaussian, the parameter ξ_2 is unity, while ξ_1 and ξ_3 are zero. Thus, the parameter ξ_2 quantifies the dominance of the long-range electrostatic interaction to the hydration free energy. Indeed, this parameter is unity in continuum solvation models such as PB (Poisson−Boltzmann) or GB (generalized Born) models[29,30] which consider only the electrostatic interaction and do not take into account the detailed short-range solvation structure. In this case, $\delta\mu_q$ becomes parabolic, i.e., proportional to the square q^2 of the net charge q of the solute. The parameters ξ_1, ξ_2, and ξ_3 can in principle be calculated using the 3D-RISM-SCF theory by extending the method developed in ref 27, but in the present work, they were estimated on the basis of the polynomial fit to $\delta\mu_q(\lambda)/|\delta\mu_q|$ (Figure 5).

We find that the Gaussian approximation describes better the electrostatic contribution to the hydration free energy for more highly charged solute species. In fact, we obtain $\xi_2 = 0.756$ for $H_3P_2O_7^-$, 0.819 for $H_2P_2O_7^{2-}$, and 0.865 for $HP_2O_7^{3-}$ for pyrophosphates, and $\xi_2 = 0.791$ for $H_2PO_4^-$, 0.852 for HPO_4^{2-}, and 0.889 for PO_4^{3-} for phosphates; i.e., the parameter ξ_2 gets closer to unity as the net charge increases. This indicates the dominance of the long-range electrostatic interaction to the hydration free energies of highly charged phosphate compounds. This accounts for the hydration free energies of charged phosphates and pyrophosphates with different dissociated states which are almost linear when plotted versus q^2 (Figure 6). The near-q^2 dependence of the hydration free energy of the multiply charged phosphates explains why the reactants in the reactions C and D are much more stabilized by hydration than the products.

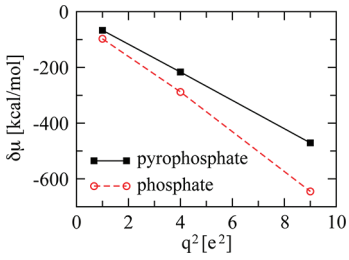

Figure 6. Hydration free energy $\delta\mu$ versus the square of the net charge q^2.

Overall, the solvation free energy is governed by the short-range hydrogen bonding effects for low-charged phosphate species, while it is dominated by the long-range electrostatic interactions for high-charged species. The 3D-RISM theory properly takes into account the molecular nature of the solute species, and this is essential for a quantitative estimate of the short-range effects such as the hydrogen bonding. In addition, since the molecular geometry is properly taken into account, the 3D-RISM theory reproduces the long-range electrostatic effect without the use of adjustable parameters such as molecular radius which are necessary in continuum model for solvation. Furthermore, it is noted that the 3D-RISM calculation result is regardless of the choice of the closure relation. In fact, we obtained essentially the same result when we used the conventional HNC closure instead of the Kovalenko−Hirata (KH) closure used in the present work (see Methods section). In particular, the near Gaussian nature of the solvation free energy for high-charged species shown in Figure 5 is not dependent on the specific use of the KH closure.

CONCLUSIONS

We investigated the hydrolysis reaction of pyrophosphate, a model compound of ATP, by using the 3D-RISM-SCF theory. Four different charged states of the pyrophosphate were considered for which experimental data for the reaction free energies are available. The hydrolysis free energies based on the gas phase results are significantly deviated from the experimental data. Taking into account the hydration effect by the 3D-RISM-SCF theory, on the other hand, predicts the experimental results of the reaction free energy with quantitative agreement for all charged states of the pyrophosphates, indicating that the solvation free energy plays a dominant role in determining the reaction free energy produced by the pyrophosphate hydrolysis.

Our results suggest that the hydration free energies of the phosphates and pyrophosphates are governed by different natures of the solute−solvent interactions depending on their charged state: the free energy of neutral states is mainly subjected to rather short-range hydrogen-bonds between the phosphates and water, while that of highly negative charged states is dominated by the long-range electrostatic interactions which give rise to a nearly parabolic behavior in the hydration free energy with respect to solute charges. The parabolic behavior of the hydration free energy is the physical origin for why the hydrolysis reaction of highly charged pyrophosphates becomes moderately exothermic. We thus provide quantitative and unambiguous evidence on the critical role of water in determining the ATP hydrolysis free energy.

Concerning the ATP hydrolysis reaction, the role of water is of interest structurally and thermodynamically not only in the reactant and product states, but also in all species along the reaction pathway.[31−33] In particular, it is challenging to characterize the transition state whose activation free energy can be very large in the nonenzymatic hydrolysis. The 3D-RISM-SCF theory, which can be applied also for these states along the reaction coordinate, will be a promising tool for a comprehensive understanding of the reaction mechanism.

METHODS

3D-RISM-SCF Theory. Since the 3D-RISM-SCF theory has already been detailed,[23−25] only a brief outline of the theory is provided here. The 3D-RISM-SCF theory combines the *ab initio* quantum chemistry method with the statistical mechanical theory of molecular solvation. In this method, the aqueous-phase free energy G_{aq} is given by a sum of the solute kinetic-energy contribution G_{kin}, the solute energy in the gas phase E_{gas}, the electronic reorganization energy δE, and the solvation free energy (excess chemical potential) $\delta\mu$:

$$G_{aq} = G_{kin} + E_{gas} + \delta E + \delta\mu \quad (1)$$

dx.doi.org/10.1021/ct300099e | J. Chem. Theory Comput. 2012, 8, 2239−2246

The solute kinetic-energy contribution G_{kin} can be evaluated from the elementary statistical mechanics. The solute energy comprises the electronic and nuclear parts:

$$E_{solute} = \langle \Psi_{solute} | H_{isolated} | \Psi_{solute} \rangle + \sum_{i,j \in solute} \frac{Z_i Z_j}{R_{ij}} \quad (2)$$

Here, Ψ_{solute}, $H_{isolated}$, Z_i, and R_{ij} denote the wave functions of solute electrons, electronic Hamiltonian of isolated solute, nuclear charge of solute atom i, and internuclear distance between solute atoms i and j, respectively. The electronic reorganization energy δE can be defined as the difference between the solute energy E_{aq} calculated with the aqueous-phase wave function Ψ^{aq}_{solute} and E_{gas} with the gas-phase wave function Ψ^{gas}_{solute}, $\delta E = E_{aq} - E_{gas}$. The solvation free energy $\delta\mu$ is determined from

$$\delta\mu = -k_B T \log \frac{\mathrm{Tr}\{e^{-\beta[V_{uv}(\mathbf{r}_u,\mathbf{r}_v)+V_{vv}(\mathbf{r}_v)]}\}}{\mathrm{Tr}\{e^{-\beta V_{vv}(\mathbf{r}_v)}\}} \quad (3)$$

Here "Tr" denotes the state sum over the solvent configurations, V_{uv} and V_{vv} are the solute−solvent and solvent−solvent interaction potentials, respectively, and r_u and r_v collectively denote the configurations of the solute and solvent molecules, respectively; and $\beta = 1/(k_B T)$ with k_B being Bolzmann's constant. The solute−solvent interaction potential V_{uv} comprises the Lennard-Jones (LJ) and electrostatic terms, $V_{uv} = V_{LJ} + V_{elec}$.

COMPUTATIONAL DETAILS

We employed the Kohn−Sham density-functional theory (KS-DFT)[34] at the B3LYP/6-31+G(d)[35] for the gas-phase solute electronic calculations using the Gaussian program.[36] Vibrational frequency calculation was done at the B3LYP/6-31+G(d) level to verify the identity of each stationary point as a minimum, and to obtain thermodynamic quantities, i.e., free energy, enthalpy, and entropy data in the gas phase. To verify the use of the B3LYP functional for our systems, we performed a MPWB1K/6-31+G(d)[37] single point energy calculation based on the B3LYP/6-31+G(d) optimized geometry. The comparison between B3LYP and MPWB1K reaction energies is summarized in Table S1 in Supporting Information.

For handling the aqueous-phase reactions, we combined the KS-DFT with the 3D-RISM theory (3D-RISM-SCF theory):[23−25] the solute electronic wave functions were determined under the influence of the water distribution function computed by the 3D-RISM theory, the 3D-RISM calculation for the water distribution function surrounding the solute molecule was carried out with the effective solute partial charges evaluated from the solute electronic wave functions, and this set of calculations was repeated until the self-consistent results were obtained. The effective partial charges on the solute atoms were determined by the restricted electrostatic potential (RESP) method.[38] The LJ parameters of the solute molecules were taken from the OPLS parameter set,[39] while the SPC model with a LJ correction for the hydrogen atom was used for the solvent parameters.[40] The water distribution function around the solute molecule can be determined by solving the 3D-RISM equation

$$h_\gamma(\mathbf{r}) = \sum_{\gamma'} \int d\mathbf{r}' c_{\gamma'}(\mathbf{r}')[w^{vv}_{\gamma'\gamma}(|\mathbf{r}-\mathbf{r}'|) + \rho_v h^{vv}_{\gamma'\gamma}(|\mathbf{r}-\mathbf{r}'|)] \quad (4)$$

with the Kovalenko−Hirata closure

$$h_\gamma(\mathbf{r}) = \begin{cases} \exp[-\beta u_\gamma(\mathbf{r}) + h_\gamma(\mathbf{r}) - c_\gamma(\mathbf{r})] - 1 & \text{for } h_\gamma(\mathbf{r}) \le 0 \\ -\beta u_\gamma(\mathbf{r}) + h_\gamma(\mathbf{r}) - c_\gamma(\mathbf{r}) & \text{for } h_\gamma(\mathbf{r}) > 0 \end{cases} \quad (5)$$

Here $h_\gamma(\mathbf{r})$ and $c_\gamma(\mathbf{r})$ refer to the 3D total and direct correlation functions of the water site γ at position r, $w^{vv}_{\gamma'\gamma}(r)$ and $h^{vv}_{\gamma'\gamma}(r)$ are the site−site intramolecular and total correlation functions of the water, ρ_v represents the average number density of water, and $u_\gamma(\mathbf{r})$ denotes the interaction potential acting on the water site γ which is generated by atoms in the solute molecule. Under the Kovalenko−Hirata closure, the following analytic expression is available for the solvation free energy:

$$\delta\mu = \rho_v k_B T \sum_\gamma \int d\mathbf{r} \left[\frac{1}{2} h_\gamma(\mathbf{r})^2 \Theta(-h_\gamma(\mathbf{r})) - c_\gamma(\mathbf{r}) - \frac{1}{2} h_\gamma(\mathbf{r}) c_\gamma(\mathbf{r}) \right] \quad (6)$$

Here $\Theta(x)$ is the Heaviside step function. The solvent density and temperature are 1.0 g/cm^3 and 298.15 K, respectively. The 3D-RISM calculations were performed on a grid of 128 × 128 × 128 points with 0.5 Å spacing. Optimized geometries in the aqueous phase of the reactants and products of the reactions A−D are presented in Figure 2, and the components of the aqueous-phase free energy G_{aq} are summarized in Table 4.

Electrostatic Contribution to the Solvation Free Energy. To express the electrostatic contribution to the solvation free energy in terms of the fluctuation of the solute−solvent electrostatic potential V_{elec}, we scale V_{elec} by a parameter λ. The resulting total interaction potential of the system shall be denoted by $V_{tot}(\lambda)$, which is given by

$$V_{tot}(\lambda) = V_{uu}(\mathbf{r}_u) + V_{vv}(\mathbf{r}_v) + V_{LJ}(\mathbf{r}_u, \mathbf{r}_v) + \lambda V_{elec}(\mathbf{r}_u, \mathbf{r}_v) \quad (7)$$

Here V_{uu} is the intrasolute interaction potential. Let us consider the solvation free energy difference $\delta\mu_q(\lambda)$ between the solvation free energy $\delta\mu(\lambda)$ of the system characterized by the parameter λ and the one $\delta\mu(\lambda = 0)$ by $\lambda = 0$ (i.e., the solvation free energy of the system in which the solute−solvent electrostatic interaction is turned off), $\delta\mu_q(\lambda) = \delta\mu(\lambda) - \delta\mu(\lambda = 0)$. Using eq 3, one obtains for $\delta\mu_q(\lambda)$

$$\begin{aligned} \delta\mu_q(\lambda) &= -k_B T \log \frac{\mathrm{Tr}\{e^{-\beta[V_{vv}(\mathbf{r}_v)+V_{LJ}(\mathbf{r}_u,\mathbf{r}_v)+\lambda V_{elec}(\mathbf{r}_u,\mathbf{r}_v)]}\}}{\mathrm{Tr}\{e^{-\beta[V_{vv}(\mathbf{r}_v)+V_{LJ}(\mathbf{r}_u,\mathbf{r}_v)]}\}} \\ &= -k_B T \log \frac{\mathrm{Tr}\{e^{-\beta V_{tot}(\lambda=0)} e^{-\beta\lambda V_{elec}}\}}{\mathrm{Tr}\{e^{-\beta V_{tot}(\lambda=0)}\}} \\ &= -k_B T \log \langle e^{-\beta\lambda V_{elec}} \rangle_0, \end{aligned} \quad (8)$$

where $\langle \cdots \rangle_0$ refers to the ensemble average taken with respect to the potential $V_{tot}(\lambda = 0)$. Using the cumulant-expansion technique,[40] $\delta\mu_q(\lambda)$ can be expanded as[27,28]

$$\delta\mu_q(\lambda) = -k_B T \sum_{n=1}^{\infty} \frac{(-\beta\lambda)^n}{n!} \langle V^n_{elec} \rangle_{0,c} \quad (9)$$

where the added subscript c in $\langle\cdots\rangle_{0,c}$ denotes the cumulant average. Explicit relations between the cumulants and the moments up to $n = 3$ are given by $\langle V_{elec}\rangle_{0,c} = \langle V_{elec}\rangle_0$, $\langle V^2_{elec}\rangle_{0,c} = \langle \delta V^2_{elec}\rangle_0$, and $\langle V^3_{elec}\rangle_{0,c} = \langle \delta V^3_{elec}\rangle_0$ where $\delta V_{elec} = V_{elec} - \langle V_{elec}\rangle_0$.[41] When rescaled by the magnitude of $\delta\mu_q = \delta\mu_q(\lambda = 1)$, one obtains the expansion

$$\delta\mu_q(\lambda)/|\delta\mu_q| = \xi_1\lambda - \xi_2\lambda^2 + \xi_3\lambda^3 + \cdots \quad (10)$$

with

$$\xi_1 = \langle V_{elec}\rangle_0/|\delta\mu_q|,$$
$$\xi_2 = \beta\langle \delta V^2_{elec}\rangle_0/(2|\delta\mu_q|),$$
$$\xi_3 = \beta^2\langle \delta V^3_{elec}\rangle_0/(6|\delta\mu_q|) \quad (11)$$

■ ASSOCIATED CONTENT

Supporting Information

Additional tables for thermodynamic data and figures for radial distribution functions of pyrophosphates. This material is available free of charge via the Internet at http://pubs.acs.org

■ AUTHOR INFORMATION

Corresponding Author

*E-mail: sihyun@sookmyung.ac.kr (S.H.), hirata@ims.ac.jp (F.H.). Phone: +82-2-710-9410 (S.H.), +81-564-55-7314 (F.H.). Fax: +82-2-2077-7321 (S.H.), +81-564-53-4660 (F.H.).

Notes

The authors declare no competing financial interest.

■ ACKNOWLEDGMENTS

We are grateful to Prof. Suzuki in Tohoku University for bringing the problem of ATP hydrolysis to our attention. We also thank Dr. Kiyota and Mr. Ogino for technical assistance. This work was supported by the Grant-in Aid for Scientific Research on Innovative Area of "Molecular Science of Fluctuations toward Biological Functions" from the MEXT in Japan. We are also grateful for the support by the grant from the Next Generation Supercomputing Project, Nanoscience Program of the ministry. This research was also supported by a grant from "Invitation Program for Advanced Research Institutions in Japan" under the Japan Society for the Promotion of Science (JSPS). This work was also supported by Basic Science Research Program through the National Research Foundation of Korea (NRF) funded by the Ministry of Education, Science and Technology (20090065791, 2011-0012096, and 2011-0026908).

■ REFERENCES

(1) Meyerhof, O.; Lohmann, K. *Biochem. Z.* **1932**, *253*, 431−461.
(2) Lipmann, F. *Adv. Enzymol.* **1941**, *1*, 99−162.
(3) Hill, T. L.; Morales, M. F. *J. Am. Chem. Soc.* **1951**, *73*, 1656−1660.
(4) Boyd, D. B.; Lipscomb, W. N. *J. Theor. Biol.* **1969**, *25*, 403−420.
(5) Albery, R. A.; Goldberg, R. N. *Biochemistry* **1992**, *31*, 10610−10615.
(6) Hayes, D. M.; Kenyon, G. L.; Kollman, P. A. *J. Am. Chem. Soc.* **1975**, *97*, 4762−4763.
(7) Hayes, D. M.; Kenyon, G. L.; Kollman, P. A. *J. Am. Chem. Soc.* **1978**, *100*, 4331−4340.
(8) Ewig, C. S.; Van Wazer, J. R. *J. Am. Chem. Soc.* **1988**, *110*, 79−86.
(9) Ma, B.; Meredith, C.; Schaefer, H. F. *J. Phys. Chem.* **1994**, *98*, 8216−8223.
(10) Hansia, P.; Guruprasad, N.; Vishveshwara, S. *Biophys. Chem.* **2006**, *119*, 127−136.
(11) Alberts, B.; Johnson, A.; Lewis, J.; Raff, M.; Roberts, K.; Walter, P. *Molecular Biology of the Cell*; Garland Science: New York, 2008.
(12) Ruben, E. A.; Plumley, J. A.; Chapman, M. S.; Evanseck, J. D. *J. Am. Chem. Soc.* **2008**, *130*, 3349−3358.
(13) Arabi, A. A.; Matta, C. F. *J. Phys. Chem. A* **2009**, *113*, 3360−3368.
(14) George, P.; Witonsky, R. J.; Trachtman, M.; Wu, C.; Dorwart, W.; Richman, L.; Richman, W.; Shurayh, F.; Lentz, B. *Biochim. Biophys. Acta* **1970**, *223*, 1−15.
(15) Hofmann, K. P.; Zundel, G. *Experimentia* **1974**, *30*, 139−140.
(16) de Meis, L. *Biochim. Biophys. Acta* **1989**, *973*, 333−349.
(17) Romero, P. J.; de Meis, L. *J. Biol. Chem.* **1989**, *264*, 7869−7873.
(18) Saint-Martin, H.; Ortega-Blake, I.; Leś, A.; Adamowicz, L. *Biochim. Biophys. Acta* **1994**, *1207*, 12−23.
(19) Colvin, M. E.; Evleth, E.; Akacem, Y. *J. Am. Chem. Soc.* **1995**, *117*, 4357−4362.
(20) Akola, J.; Jone, R. O. *J. Phys. Chem. B* **2003**, *107*, 11774−11783.
(21) Marenich, A. V.; Cramer, C. J.; Truhlar, D. G. *J. Phys. Chem. B* **2009**, *113*, 6387−6396.
(22) Tang, E.; Di Tommaso, D.; de Leeuw, N. H. *Phys. Chem. Chem. Phys.* **2010**, *12*, 13804−13815.
(23) Kovalenko, A.; Hirata, F. *J. Chem. Phys.* **1999**, *110*, 10095−10112.
(24) Sato, H.; Kovalenko, A.; Hirata, F. *J. Chem. Phys.* **2000**, *112*, 9463−9468.
(25) Yoshida, N.; Hirata, F. *J. Mol. Liq.* **2011**, *159*, 83−92.
(26) Tang, E.; Di Tommaso, D.; de Leeuw, N. H. *J. Chem. Phys.* **2009**, *130*, 234502.
(27) Chong, S.-H.; Hirata, F. *J. Chem. Phys.* **1997**, *106*, 5225−5238.
(28) Wang, L.; Friesner, R. A.; Berne, B. J. *J. Phys. Chem. B* **2010**, *114*, 7294−7301.
(29) Sharp, K. A.; Honig, B. *Annu. Rev. Biophys. Biophys. Chem.* **1990**, *19*, 301−332.
(30) Still, W.; Tempczyk, A.; Hawley, R.; Henrickson, T. *J. Am. Chem. Soc.* **1990**, *112*, 6127−6129.
(31) Wang, Y.-N.; Topol, I. A.; Collins, J. R.; Burt, S. K. *J. Am. Chem. Soc.* **2003**, *125*, 13265−13273.
(32) Rosta, E.; Kamerlin, S. C. L.; Warshel, A. *Biochemistry* **2008**, *47*, 3725−3735.
(33) Kamerlin, S. C. L.; Haranczyk, M.; Warshel, A. *ChemPhysChem* **2009**, *10*, 1125−1134.
(34) Kohn, W.; Sham, L. J. *Phys. Rev.* **1965**, *140*, A1133−A1138.
(35) Becke, A. D. *J. Chem. Phys.* **1993**, *98*, 5648−5652.
(36) Frisch, M. J.; Trucks, G. W.; Schlegel, H. B.; Scuseria, G. E.; Robb, M. A.; Cheeseman, J. R.; Montgomery, J. A., Jr.; Vreven, T.; Kudin, K.; Burant, J. C.; Millam, J. M.; Iyengay, S. S.; Tomasi, J.; Barone, V.; Mennucci, B.; Cossi, M.; Scalmani, G.; Rega, N.; Petersson, G. A.; Nakatsuji, H.; Hada, M.; Ehara, M.; Toyota, K.; Fukuda, R.; Hasegawa, J.; Ishida, M.; Nakajima, T.; Honda, Y.; Kitao, O.; Nakai, H.; Klene, M.; Li, X.; Knox, J. E.; Hratchian, H. P.; Cross, J. B.; Adamo, C.; Jaramillo, J.; Comperts, R.; Startmann, R. E.; Yazyev, O.; Austin, A. J.; Cammi, R.; Pomelli, C.; Ochterski, J. W.; Ayala, P. Y.; Morokuma, K.; Voth, G. A.; Salvador, P.; Dannenburg, J. J.; Zakrzewski, V. G.; Dapprich, S.; Daniels, A. D.; Strain, M. C.; Farkas, O.; Malick, D. K.; Rabuck, A. D.; Raghavachari, K.; Foresman, J. B.; Ortiz, J. V.; Cui, Q.; Baboul, A. G.; Clifford, S.; Cioslowski, J.; Stefanov, B. B.; Liu, G.; Liashenko, A.; Piskorz, P.; Komaromi, I.; Martin, R. L.; Fox, D. J.; Keith, T.; Al-Laham, M. A.; Peng, C. Y.; Nanayakkara, A.; Challacombe, M.; Gill, P. M. W.; Johnson, B.; Chem, W.; Wong, M. W.; Gonzalez, C.; Pople, J. A. *Gaussian 03, Revision C.02*; Gaussian, Inc.: Wallingford, CT, 2004.
(37) Ribeiro, A. J. M.; Ramos, M. J.; Fernandes, P. A. *J. Chem. Theory Comput.* **2010**, *6*, 2281−2292.
(38) Bayly, C. I.; Cieplak, P.; Cornell, W. D.; Kollman, P. A. *J. Phys. Chem.* **1993**, *97*, 10269−10280.
(39) Berendsen, H. J. C.; Grigera, J. R.; Straatsma, T. P. *J. Phys. Chem.* **1987**, *91*, 6269−6271.

(40) Pettitt, B. M.; Rossky, P. J. *J. Chem. Phys.* **1982**, *77*, 1451−1457.
(41) van Kampen, N. G. *Stochastic Processes in Physics and Chemistry*; North-Holland: Amsterdam, 1981.